Pergamon

Computers Math. Applic. Vol. 34, No. 5/6, pp. 559–570, 1997

0898-1221/97 $17.00 + 0.00

PII: S0898-1221(97)00153-3

Application of Extension Theory to Antiproton-Nucleon Systems with Continuous Set of Resonances in Annihilation Channel

YU. A. KUPERIN AND S. B. LEVIN
Laboratory of the Complex Systems Theory
Institute for Physics, St. Petersburg State University
St. Petersburg, 198904, Russia

YU. B. MELNIKOV
International Solvay Institutes for Physics and Chemistry
Campus Plane, ULB
C.P. 231, Bd. du Triomphe, B-1050, Brussels, Belgium

E. A. YAREVSKY
Laboratory of the Complex Systems Theory
Institute for Physics, St. Petersburg State University
St. Petersburg, 198904, Russia

Abstract—The exact expressions for scattering length and partial total cross-section for $\bar{p}n$ and $\bar{p}p$ systems are obtained in the frame of the extended Hilbert space model with continuous spectrum of resonances treated as an annihilation channel. The numerical algorithm for scattering data calculation is suggested. The numerical calculations for $\bar{p}n$ and $\bar{p}p$ scattering data at angular momentum $L = 0, 1, 2, 3$ are performed on this base. The interaction parameters are fitted via two-body scattering data. A satisfactory agreement between experimental and theoretical data is obtained.

Keywords—Annihilation, Continuous spectrum, Resonances, Self-adjoint extensions, Boundary value problem, Scattering length, Cross-sections.

1. INTRODUCTION

Few-body systems with antiprotons are nowadays the subject of intensive investigations [1–4]. Such systems include more information about particle structure and interparticle interaction. But the properties of such systems are more complicated than ones for systems without antiparticles. There is no annihilation description from the QCD point of view because the annihilation region coincides with the nonperturbative QCD one. Because of the complication of the processes which include antiparticles, there are a lot of physical models for such process description.

The main annihilation models are the different variants of optical potential models [5,6], coupling channel models [7,8], quark models [9,10], and others. The optical potential models lead to the non-self-adjoint system Hamiltonians. This non-self-adjointness is a reason for many

We are very grateful to O. D. Dalkarov and A. E. Kudrjavtsev for fruitful discussions and interesting remarks. We thank the Commission of the European Communities for the financial support in the frame of EC-Russia Collaboration Contract ESPRIT P 9282 ACTCS. The research described in this publication was made possible in part by Grant # NX 1000 from the International Science Foundation.

Typeset by $\mathcal{A}_{\mathcal{M}}\mathcal{S}$-TeX mathematical and computational difficulties. Moreover, more detail characteristics of scattering processes, for instance polarization ones, are not described by these models satisfactorily. The quark models are strongly dependent on from effective annihilation operator choice and diagram hierarchy. The coupling channel models contain a large arbitrariness for channel coupling operators, but they show the best experimental data description.

There is a satisfactory description of the basic experimental scattering data for all these models. The total and differential elastic and annihilation cross-sections and scattering lengths are reproduced with acceptable accuracy. But only certain approaches allow us to calculate exactly the more delicate characteristics such as, for instance, differential rearrangement cross-sections of scattering process $\bar{p}p \to \bar{n}n$ [11].

Moreover, the recent developments of $\bar{p}$-physics allows us to attack theoretically the few-body systems with $\bar{p}$. For example, the important problem is the study of $\bar{p}d$-scattering. The precise analysis of this system allows us in particular to extract the unknown data about the $\bar{n}n$ process [2]. The other reason is the study of weakly-coupled bound states for $\bar{p}dd$, $\bar{p}pd$-systems, and some others [12,13]. The annihilation effects may be rather large in such systems [13].

In the present work, we suggest a model for $\bar{p}N$ scattering with annihilation channel which is treated as the continuous spectrum of resonances or as the continuous spectrum of a trial Hamiltonian in some auxiliary Hilbert space. We restrict ourselves to consideration of two-body systems only, namely, $\bar{p}p$ and $\bar{p}n$. The main goal of the paper is to construct the annihilation interaction as well as nuclear ones for systems in frames of the well-developed extended Hilbert space approach [14–16]. It opens the way to attack three-body problems mentioned above because one needs for this purpose $\bar{p}p$ and $\bar{p}n$ interactions as input data. On the other hand, using the $\bar{p}N$-interaction, we calculate more delicate characteristics of the $\bar{p}N$ systems such as the ratio of real to imaginary part of the elastic scattering amplitude, Argand diagrams for lowest partial waves, and some others.

The paper is organized as follows. In Section 2, we briefly describe the mathematical model laying in the background of our consideration. We modify the original extended Hilbert space approach [14–16] for continuous spectrum of the auxiliary Hamiltonian following [17]. In Section 3, we reduce the problem in question to some well-posed boundary value problem having the spectral parameter in the boundary conditions. We also derive some explicit formulas for scattering data. It makes a sound base for numerical analysis described in Section 4. We present in this section the results of numerical calculations.

2. DESCRIPTION OF THE MODEL

In the present paper, we treat strong interacting particles as composites having complicated internal structure. In order to take into account this internal structure, we separate the role of different degrees of freedom in the two-particle system. Namely, in asymptotics regimes when two composites are far from each other, we describe the dynamics of the two-body system by ordinary two-body quantum Hamiltonian $H^{\mathrm{ex}} = -\Delta + V$ with some potential. It means that internal degrees of freedom are frozen and do not play any role. On the other hand, when particles strongly interact, i.e., they are close to each other, the internal degrees of freedom play an essential role and should be incorporated into dynamics.

It is clear that this incorporation is impossible in the frame of the same Hilbert space where the Hamiltonian H^{ex} acts, and one needs to add some auxiliary Hilbert space $\mathcal{H}^{\mathrm{in}}$ taking into account additional (internal) degrees of freedom. Let H^{in} be the Hamiltonian which governs the dynamics in $\mathcal{H}^{\mathrm{in}}$. Then the operator $H^{\mathrm{ex}} \oplus H^{\mathrm{in}} = H$ generates two independent dynamics into the channels $\mathcal{H}^{\mathrm{ex}} \oplus \mathcal{H}^{\mathrm{in}} = \mathcal{H}$. To switch on the interaction between external and internal degrees of freedom, we do the following. First, we restrict both operators H^{ex} and H^{in} to some symmetric operators H_0^{ex} and H_0^{in} acting in $\mathcal{H}^{\mathrm{ex}}$ and $\mathcal{H}^{\mathrm{in}}$, respectively. Second, we combine them into the direct sum $H_0 = H_0^{\mathrm{ex}} \oplus H_0^{\mathrm{in}}$ being the symmetric operator again. And finally, we construct the total Hamiltonian H_Γ describing the common dynamics of external and internal degrees of freedom as the self-adjoint extension of H_0. One can treat then the difference

$$H_\Gamma - H \equiv W \tag{1}$$

as the interaction between $\mathcal{H}^{\text{ex}}$ and $\mathcal{H}^{\text{in}}$ channels.

The scheme described above has been developed in a series of papers [14–16,18] for the case when the spectrum σ^{ex} of H^{ex} has both continuous and discrete components but the spectrum σ^{in} of H^{in} has the discrete component only. This scheme has been applied to various physical problems where the discrete eigenvalues of H^{in}, being real before the restriction of H^{in} to the symmetric H_0^{in}, became the set of resonances for the H^{ex} after self-adjoint extension and simultaneous "exclusion" of the internal channel $\mathcal{H}^{\text{in}}$.

The first attempt to apply the mathematical approach described above to the annihilation processes has been done in [17] for the case of continuous spectrum of H^{in}. When it is the case, it was shown that the continuous spectrum of H^{in}, being real because H^{in} is self-adjoint operator, became the continuous spectrum of resonances for H^{ex} again after self-adjoint extension of H_0 and the "exclusion" procedure. At the same time for the total Hamiltonian H_Γ, the continuous spectrum of H^{in} generates the real spectrum with thresholds which are the thresholds for different annihilation processes.

Here we apply the technique of extended Hilbert spaces to the $\bar{p}p$ and $\bar{p}n$ scattering with annihilation channels. In the next section, we describe the realization of this technique for $\bar{p}N$ systems and reduce the abstract operator description to the well-posed boundary value problem for the differential equation.

3. BOUNDARY PROBLEM AND SCATTERING DATA

Let us briefly describe the construction of the model Hamiltonian H_Γ (for details, see [14,17]). First consider the "external" block of the Hamiltonian H^{ex} in the Hilbert space $\mathcal{H}^{\text{ex}} = L^2(\mathbf{R}^3)$. For the $\bar{p}n$ system we take H^{ex} as the Laplace operator, $H^{\text{ex}} = -\Delta$, and for the $\bar{p}p$ system we add the Coulomb attraction, $H^{\text{ex}} = -\Delta + ar^{-1}$, where $a = M_p e_p e_{\bar{p}}$ is the Coulomb constant. Next we introduce an abstract Hilbert space $\mathcal{H}^{\text{in}}$ where an additional self-adjoint operator H^{in} acts. In the simplest case of our model, H^{in} is given by its spectral measure dE_ζ (which is the parameter of the model),

$$H^{\text{in}} = \int_{-M}^{\infty} \zeta \, dE_\zeta. \tag{2}$$

Here $-M$ is the annihilation threshold, $M = m_{\bar{p}} + m_{n(p)} - \sum_i m_i$, where $\sum_i m_i$ is the sum of annihilation products masses. The operator H^{in} describes the annihilation channels. In the more general case, its spectrum can also include some eigenvalues interpreted as binding energies of quark compound bag [17,18]. Next, both self-adjoint operators H^{ex} and H^{in} are restricted to symmetric one, H_0^{ex} and H_0^{in}, respectively. For the "external" channel $L^2(\mathbf{R}^3)$, the operator H_0^{ex} is determined on the $W_2^2(\mathbf{R}^3)$ functions, vanishing in the vicinity of the sphere S_ρ of radius ρ. This sphere is called the interaction surface, and ρ is the annihilation radius. For additional channel $\mathcal{H}^{\text{in}}$, we use a special scheme of restriction described in detail in various papers [14–18]. The common extension of the symmetric operator $H_0^{\text{ex}} \oplus H_0^{\text{in}}$ to some self-adjoint operator H_Γ gives the total Hamiltonian of the system. The correspondent theory and calculations are given in detail in [14,17]. In the present paper, we use the results of [17] which allow us to restrict the spectral problem for H_Γ to the effective boundary problem in $\mathbf{R}^3$:

$$H_\Gamma \Psi = z\Psi, \tag{3.1}$$

$$\Psi^+(r, s; z)|_{r=\rho} = \Psi^-(r, s; z)|_{r=\rho}, \tag{3.2}$$

$$[\Psi'(r, s; z)]\,|_{r=\rho} = -Q(z) \int_{S_\rho} \Psi(\rho, s'; z)\, \bar{\Phi}(s')\, ds' \Phi(s), \tag{3.3}$$

where $(r,s) = x \in \mathbf{R}^3$ are spherical coordinates, $\Psi^{\pm}(r,s;z) = \Psi(r \pm 0, s; z)$, $\Psi' = \frac{\partial \Psi}{\partial r}$, $[\Psi]|_{r=\rho} = \Psi^+|_{r=\rho} - \Psi^-|_{r=\rho}$. Function $\Phi(s) \in L^2(S_\rho)$ is the channel coupling function (parameter of the model), and its L^2-norm $\|\Phi\|^2 = \int_{S_\rho} |\Phi(s)|^2 \, ds$ is the coupling constant. The energy-dependent function $Q(z)$ is given by the Schwarz integral [11–17]

$$Q(z) = \int_{-M}^{\infty} \frac{\eta^2 + z\zeta}{\zeta - z} \, d\mu(\zeta),$$

where the constant $\eta^2 \in \mathbf{R}$ is the model parameter, and the absolute continuous measure $d\mu(\zeta)$ is calculated in terms of the spectral measure dE_ζ. Its derivative $\mu'(\zeta) = \frac{d\mu(\zeta)}{d\zeta}$ has the sense of velocity of annihilation probability alteration depending on energy.

Note, that in the general case the obtained Hamiltonian is determined by the boundary value problem (3) and cannot be represented in the matrix form $\begin{pmatrix} H^{ex} & B \\ B^* & H^{in} \end{pmatrix}$ in the Hilbert space $L^2(\mathbf{R}^3) \oplus \mathcal{H}^{in}$, whereas any operator of the latter form can be obtained in frames of the used operator extension theory method [14].

Effective energy-dependent self-adjoint boundary conditions (3.2),(3.3) simulate the short-range nuclear interaction including the annihilation channel with threshold $-M$. Note, that in the limit case $\|\Phi\| = 0$, the channels are disjoint and we have the free (or Coulomb) motion in $\mathbf{R}^3$, whereas for $\|\Phi\| = \infty$, the system is equivalent to the scattering by hard core of radius ρ.

After partial analysis of the boundary value problem (3.1)–(3.3), we obtain the following boundary problem in the l^{th} partial wave ψ_l:

$$\begin{aligned}
&\left(-\partial_r^2 + l(l+1)r^{-2}\right)\psi_l(r,z) = z\psi_l(r,z), && \text{for } \bar{p}n \text{ system},\\
&\left(-\partial_r^2 + l(l+1)r^{-2} + ar^{-1}\right)\psi_l(r,z) = z\psi_l(r,z), && \text{for } \bar{p}p \text{ system},\\
&\psi_l^+(r,z)|_{r=\rho} = \psi_l^-(r,z)|_{r=\rho}, &&\\
&[\psi_l'(r,z)]|_{r=\rho} = -(2l+1)|\phi_l|^2 Q(z)\psi_l(r,z)|_{r=\rho}, &&
\end{aligned}$$

where ϕ_l are the partial components of the coupling function $\Phi(s)$. Let us represent $\psi_l^{\pm}(r,z)$ as follows [19]:

$$\psi_l^+(kr) = \frac{i^l}{2\pi}\left[h_l^-(kr) + S_l(k)h_l^+(kr)\right], \tag{4.1}$$

$$\psi_l^-(kr) = C_l(k) f_l^r(kr), \tag{4.2}$$

where $z = k^2$ and

$$h_l^{\pm}(x) = f_l^r(x) \pm i f_l^s(x),$$

$f_l^r(x)$ and $f_l^s(x)$ are regular and singular partial solutions of the equation (3.1), $S_l = e^{2i\delta_l}$ is S-matrix element.

Substituting (4.1) and (4.2) in (3.1) and (3.2), one can express S_l as:

$$S_l(k) = \frac{\left[|\phi_l|^2 Q\left(k^2\right) - f_l^{r\prime}(k\rho)/f_l^r(k\rho)\right] h_l^-(k\rho) + h_l^{-\prime}(k\rho)}{\left[-|\phi_l|^2 Q\left(k^2\right) + f_l^{r\prime}(k\rho)/f_l^r(k\rho)\right] h_l^+(k\rho) - h_l^{+\prime}(k\rho)}, \tag{5}$$

where primes designate derivatives. In the frame of our model, one can calculate the scattering length for the $\bar{p}n$ system,

$$a_0 = \frac{\rho^2 Q(0)|\phi_l|^2}{\rho Q(0)|\phi_l|^2 - 1}, \tag{6}$$

and for the $\bar{p}p$ system,

$$a_0^c = -\lim_{k\to 0}\left[C_0^2(\zeta)k \operatorname{cotan}\left(\delta_0(k)\right) + ah(\zeta)\right]^{-1},$$

where

$$C_0^2(\zeta) = \frac{2\pi\zeta}{e^{2\pi\zeta} - 1}, \qquad \zeta = -\frac{a}{2k},$$

$$h(\zeta) + \ln(\zeta) = \zeta^2 \sum_{j=1}^{\infty} \frac{1}{j(j^2 + \zeta^2)} - \gamma,$$

and γ stands for the Euler constant.

Using asymptotic expansions for regular $f_0^r(x) \equiv F_0(x)$ and singular $f_0^s(x) \equiv G_0(x)$ Coulomb functions at $x \to 0$,

$$F_0(kr) = \left(\sqrt{\frac{2}{\pi}}\, C_0\right) kr \left(1 + \zeta kr - \frac{1}{6}\, k^2r^2 + \frac{1}{3}\, \zeta^2 k^2 r^2 + \cdots\right),$$

$$G_0(kr) = -\left(\sqrt{\frac{2}{\pi}}\, \frac{1}{C_0}\right) \left\{1 + 2kr\zeta(\ln(2kr) + 2\gamma - 1 + h(\zeta) + \ln\zeta) - \frac{k^2r^2}{2} + 3\zeta^2 k^2 r^2 + \cdots\right\},$$

in the first order of perturbation theory with respect to parameter $\alpha \equiv a/2$ ($\alpha = 0.035\, fm^{-1}$ for $\bar{p}p$ system) we have:

$$a_0^c \approx \frac{-1 + \alpha\rho}{1/\rho^2 Q(0) - 1/\rho + 2\alpha[\ln(2\alpha\rho) + 2\gamma - 1] + \alpha/Q(0)(2/\rho - 1/\rho(1 - \alpha\rho))}. \tag{7}$$

Let us investigate the dependence of partial cross-section $\sigma_l(k)$ on the coupling constant $|\phi_l|^2$:

$$\sigma_l = 4\pi |f_l|^2 = 4\pi \left|\frac{1 - S_l}{2ik}\right|^2. \tag{7'}$$

Using the expression (5), we have for $4k^2\sigma_l(k, |\phi|^2) = |1 - S_l|^2$:

$$4k^2\sigma\left(k, |\phi|^2\right) = \frac{|\phi|^4 \left|Q\left(k^2\right)\right|^2 \left(3f_r^2 - f_s^2\right) - 2g|\phi|^2 \operatorname{Im}\left(Q\left(k^2\right) h^+\right) - g^2}{|\phi|^4 \left|Q\left(k^2\right)\right|^2 \left(f_r^2 + f_s^2\right) + 2g|\phi|^2 \operatorname{Im}\left(Q\left(k^2\right) h^+\right) + g^2} + 1, \tag{8}$$

where $g = f_s' - f_r' f_s/f_r$. Then

$$4k^2 \frac{\partial\sigma\left(k, |\phi|^2\right)}{\partial\left(|\phi|^2\right)} = \frac{8|\phi|^2 \left|Q\left(k^2\right)\right|^2 f_r^2 g \operatorname{Im}\left(Q\left(k^2\right) h^+\right) \left(|\phi|^2 + g/\operatorname{Im}\left(Q\left(k^2\right) h^+\right)\right)}{\left(|\phi|^4 \left|Q\left(k^2\right)\right|^2 \left(f_r^2 + f_s^2\right) + 2g|\phi|^2 \operatorname{Im}\left(Q\left(k^2\right) h^+\right) + g^2\right)^2}.$$

Therefore, the partial cross-section has the point of maximum with respect to the coupling constant at

$$|\phi_l^{\max}|^2 = -\frac{g_l}{\operatorname{Im}\left(Q\left(k^2\right) h_l^+\right)} = \frac{f_l^{r\prime}/f_l^r - f_l^{s\prime}/f_l^s}{\operatorname{Re}\left(Q\left(k^2\right)\right) + \operatorname{Im}\left(Q\left(k^2\right)\right) f_l^r/f_l^s}.$$

In the hard core case $|\phi_l|^2 = \infty$ for any l, equation (8) turns into

$$\sigma_l^h(k) = \frac{\pi}{k^2}\left(1 + \frac{3f_l^{r2} - f_l^{s2}}{f_l^{r2} + f_l^{s2}}\right). \tag{9}$$

In the model described above, the boundary condition (3.3) includes the nuclear and annihilation effects simultaneously. The more realistic description of $\bar{N}N$ short-range interaction supposes the separation of annihilation and nuclear interaction radii.

In the frame of our model, we have included the nuclear interaction by means of additional self-adjoint boundary conditions on the sphere of radius R:

$$[\partial_n \Psi]|_{r=R} = \nu \Psi|_{r=R}, \tag{10}$$

where ν is the function from $L^2(\mathbf{S}_R)$. We defined the annihilation interaction by means of previous energy-dependent boundary conditions on the sphere of radius ρ. Therefore, the new boundary problem has the form

$$H_\Gamma \Psi = z\Psi, \tag{11.1}$$

$$\Psi^+(r,s;z)|_{r=R} = \Psi^0(r,s;z)|_{r=R}, \tag{11.2}$$

$$[\Psi'(r,s;z)]\,|_{r=R} = \nu\Psi(R,s;z), \tag{11.3}$$

$$\Psi^0(r,s;z)|_{r=\rho} = \Psi^-(r,s;z)|_{r=\rho}, \tag{11.4}$$

$$[\Psi'(r,s;z)]\,|_{r=\rho} = -Q(z)\Phi(s)\int_{S_\rho} \Psi(\rho,s';z)\,\bar{\Phi}(s')\,ds', \tag{11.5}$$

where the function $\Psi^+(r) \equiv \Psi(r)|_{R<r<\infty}$, the function $\Psi^0(r) \equiv \Psi(r)|_{\rho<r<R}$, and the function $\Psi^-(r) \equiv \Psi(r)|_{0<r<\rho}$, $[\Psi]|_{r=r^*} = \Psi|_{r=r^*+0} - \Psi|_{r=r^*-0}$, where $r^* = R$ or $r^* = \rho$.

After the partial analysis we obtain the following boundary problem in the l^{th} partial wave ψ_l:

$$\begin{aligned}
&\left(-\partial_r^2 + l(l+1)r^{-2}\right)\psi_l(r,z) = z\psi_l(r,z), && \text{for the } \bar{p}n \text{ system},\\
&\left(-\partial_r^2 + l(l+1)r^{-2} + ar^{-1}\right)\psi_l(r,z) = z\psi_l(r,z), && \text{for the } \bar{p}p \text{ system},\\
&\psi_l^+(r,z)|_{r=R} = \psi_l^0(r,z)|_{r=R},\\
&[\psi_l'(r,z)]\,|_{r=R} = \nu_l\psi_l(r,z)|_{r=R},\\
&\psi_l^0(r,z)|_{r=\rho} = \psi_l^-(r,z)|_{r=\rho},\\
&[\psi_l'(r,z)]\,|_{r=\rho} = -(2l+1)|\phi_l|^2 Q(z)\psi_l(r,z)|_{r=\rho},
\end{aligned}$$

where ϕ_l are the partial components of the coupling function $\Phi(s)$ and ν_l are the partial components of the function $\nu(s)$. Let us represent $\psi_l^{\pm}(r,z)$ and ψ_l^0 as follows [19]:

$$\psi_l^+(kr) = \frac{i^l}{2\pi}\left[h_l^-(kr) + S_l(k)h_l^+(kr)\right], \tag{12.1}$$

$$\psi_l^0(kr) = C_l^1(k)f_l^r(kr) + C_l^2(k)f_l^s(kr), \tag{12.2}$$

$$\psi_l^-(kr) = C_l^3(k)f_l^r(kr), \tag{12.3}$$

where $h_l^{\pm}(x) = f_l^r(x) \pm i\,f_l^s(x)$, $f_l^r(x)$ and $f_l^s(x)$ are regular and singular partial solutions of the equation (11.1), $S_l = e^{2i\delta_l}$ is the partial S-matrix element.

As it was performed in the previous model, one can express S_l as:

$$S_l(k) = \frac{h_l^-(kR)\Omega_l(k,R,\rho) + h_l^{-\prime}(kR)}{-h_l^+(kR)\Omega_l(k,R,\rho) - h_l^{+\prime}(kR)}, \tag{13}$$

where

$$\Omega_l(k,R,\rho) \equiv \frac{f'^r_l D_l(k\rho) - f'^s_l(kR)}{f_l^s(kR) - f_l^r(kR)D_l(k\rho)} - \nu_l,$$

$$D_l(k\rho) \equiv \frac{f'^s_l(k\rho)/B_l(k\rho) - f_l^s(k\rho)}{f'^r_l(k\rho)/B_l(k\rho) - f_l^r(k\rho)},$$

$$B_l(k\rho) \equiv \frac{f_l'^{r}}{f_l^r} - |\phi_l|^2 Q(z),$$

and primes designate derivatives.

In the frame of the model, one can calculate the scattering length a for the $\bar{p}n$ system,

$$a = R - \frac{1}{1/(R-\hat{a}) + \nu_0}, \tag{14}$$

where

$$\hat{a} = \rho - \frac{1}{1/\rho - Q(0)|\phi_0|^2}.$$

The scattering length for the $\bar{p}p$ system can be calculated as it has been performed for the model with one boundary condition.

4. NUMERICAL ANALYSIS

The models described in the previous section include a set of parameters. These parameters may be defined only by the comparison of the theoretical and known experimental data. The obtained interaction may be used for the calculation of the unfitted observables. Therefore, such calculation allows us to verify a "quality" of the interaction. In this section, we describe the fitting procedure and discuss some obtained results.

In the model with one boundary condition (3), there are the following parameters: the interaction radius ρ, coupling constants $|\phi_l|^2$, the extension parameter η^2, and the functional measure parameter $\mu(\zeta)$. The model with two boundary conditions (11) includes in addition the second interaction radius R and coupling constants ν_l. Numerical experiment shows that the description of experimental data weakly depends on the choice of $\mu(\zeta)$ form, if the measure is normalized. Therefore it is possible to choose the measure in the simple and convenient form:

$$\mu(\zeta) = \frac{\beta - M}{\beta} \frac{\zeta}{\zeta + \beta}.$$

This representation includes only one parameter β.

All used model parameters can be fitted via experimental data, such as complex scattering length and total scattering cross-section. Let us introduce the functional

$$\chi = \frac{1}{k_{\max} - k_{\min}} \int_{k_{\min}}^{k_{\max}} \frac{|\sigma_{\rm tot}(k) - \sigma_{\rm tot}^{\rm exp}(k)|}{\sigma_{\rm tot}(k) + \sigma_{\rm tot}^{\rm exp}(k)} dk,$$

where $\sigma_{\rm tot}(k) = \sum_l (2l+1)\sigma_l^t$ and σ_l^t are given by the relation:

$$\sigma_l^t = 4\pi|f_l|^2 = \frac{\pi}{k^2}|1 - S_l|^2 + \frac{\pi}{k^2}\left(1 - |S_l|^2\right). \tag{15}$$

For the experimental total cross-section $\sigma_{\rm tot}^{\rm exp}$, we use the parameterizations performed in [20,21]. The $\bar{p}p$ total cross-section one is fitted by experimental data [20] as

$$\sigma_{\rm tot}^{(\bar{p}p)}(k) = 65.55 + \frac{53.84}{k}. \tag{16}$$

For the $\bar{p}n$ total cross-section, the parameterization is evaluated on the base of experimental $\bar{p}d$ data [21] as follows:

$$\sigma_{\rm tot}^{(\bar{p}n)}(k) = 60.59 + \frac{44.26}{k}. \tag{17}$$

Table 1. The parameterization results for $\bar{p}n$ interaction.

Waves	χ	ρ, fm	η^2, fm^{-2}	β, $\times 10^3$ fm^{-1}	$\lvert\phi_0\rvert^2$	$\lvert\phi_1\rvert^2$	$\lvert\phi_2\rvert^2$	$\lvert\phi_3\rvert^2$
s	12.63	0.60	80000	5005	5.83	–	–	–
$s+p$	3.56	0.90	1200	203	11.9	4.5	–	–
$s+p+d$	0.34	1.20	600	42	3.83	14.0	12.0	–
$s+p+d+f$	0.09	1.15	5000	57	0.64	3.0	7.0	7.0

Table 2. The parameterization results for $\bar{p}p$ interaction.

Waves	χ	ρ, fm	η^2, fm^{-2}	β, $\times 10^3$ fm^{-1}	$\lvert\phi_0\rvert^2$	$\lvert\phi_1\rvert^2$	$\lvert\phi_2\rvert^2$	$\lvert\phi_3\rvert^2$
s	12.15	0.65	30000	2367	7.0	–	–	–
$s+p$	3.80	1.05	150	85	35.0	8.1	–	–
$s+p+d$	0.90	1.35	12	32	122.0	20.0	2.0	–
$s+p+d+f$	0.11	1.59	470	20	1.6	9.0	1.1	1.2

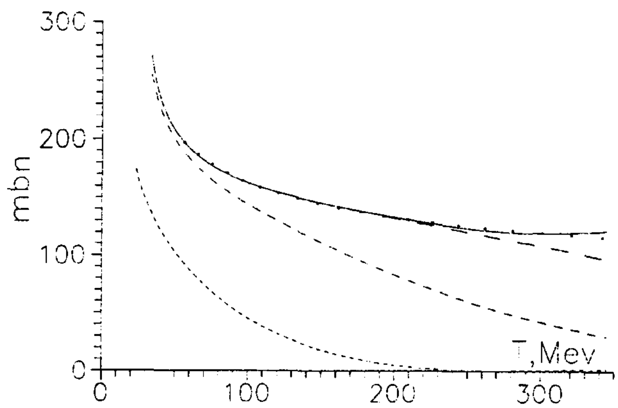

Figure 1. The total $\bar{p}n$ cross-section for the model with one radius of interaction. Solid line is for the model with S, P, D, and F waves, long-dashed line is for the model with S, P, and D waves, short-dashed line is for the model with S and P waves, dotted line is for the model with S wave only. The experimental values are taken from [2].

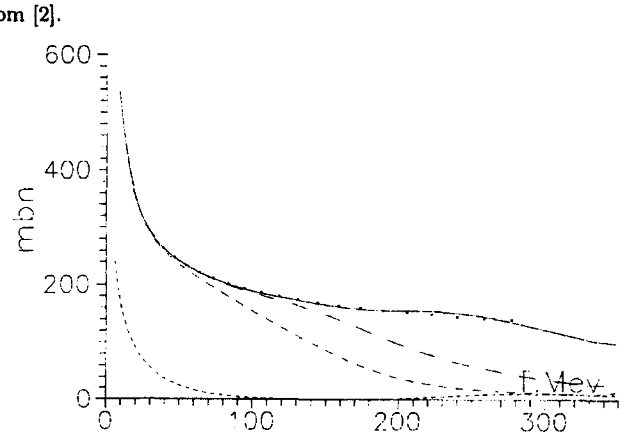

Figure 2. The total $\bar{p}p$ cross-section for the model with one radius of interaction. The notations are the same as for Figure 1.

In the case where the momentum transfer k of $\bar{p}$ in equations (16),(17) is measured in Gev/c then $\sigma_{\rm tot}^{(\bar{p}N)}(k)$ is measured in mbn.

By using the complex scattering length, we fix two parameters, namely, β and η^2. We use the same value $a_0 = (-0.93 + i0.95)$ fm [2] of the scattering length both for $\bar{p}p$ and $\bar{p}n$ because the

Coulomb difference is rather small and its exact value is unknown. After the elimination of β and η^2, we minimize the functional χ as a function of the other parameters in the momentum region $k_{\min} = 50\,\mathrm{Mev}/c$, $k_{\max} = 300\,\mathrm{Mev}/c$.

The results of the calculation of the model parameters for $\bar{p}n$ and $\bar{p}p$ systems are shown in the Table 1 and Table 2, respectively. The total cross-section for various number of partial waves are demonstrated in Figure 1 and Figure 2. The calculated results in the Figures 1 and 2 show that the role of F-wave both in $\bar{p}p$ and $\bar{p}n$ cases is small enough. This fact allows us to limit our consideration by S, P, D, and F waves only.

The total cross-section has the resonance behavior near threshold. This fact confirms the prediction of Shapiro and coauthors [7,8] about existence of near threshold resonances, so-called barionium states.

The existence of an annihilation channel in the system brings the great difference in comparison with the experimental data of NN scattering. It is reflected, for example, in a behavior of higher partial waves. As it was noted in [2], the P-waves contribute 40–60% in the total cross-section. This contribution can be traced to the behavior of the ratio of real to imaginary part of the elastic scattering forward amplitude τ as a function of $\bar{p}$-momentum transfer (see Figure 3). This ratio rapidly increases from -1 at the threshold up to 0 at $200\,\mathrm{Mev}/c$. The reason for that is connected with the compensation of real parts of S- and P-wave amplitudes, which have the different signs [7,8] (see the Argand diagrams for S- and P-waves in Figure 4).

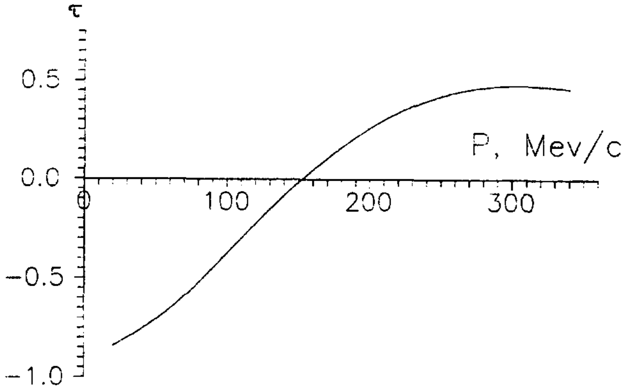

Figure 3. The ratio τ of real to imaginary part of the elastic scattering forward amplitude as a function of $\bar{p}$-momentum transfer for the model with one radius of interaction.

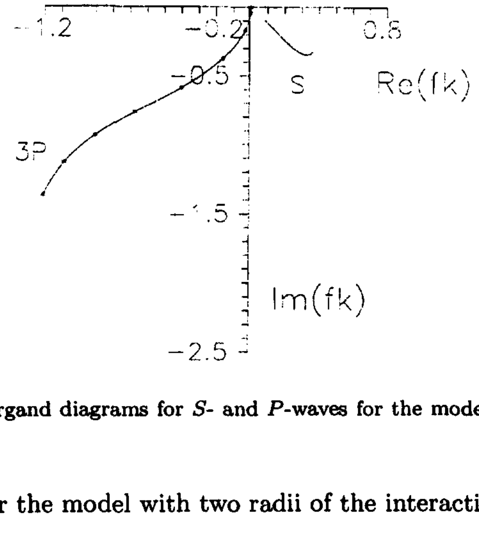

Figure 4. The Argand diagrams for S- and P-waves for the model with one radius of interaction.

The fitted parameters for the model with two radii of the interaction for $\bar{p}p$ system are shown in Table 3 and Figure 5.

Table 3. The parameterization results for $\bar{p}p$ interaction with separated radii.

Waves	s	$s+p$	$s+p+d$	$s+p+d+f$
χ	16.40	3.72	0.66	0.51
ρ, fm	0.60	0.11	0.11	0.09
R, fm	1.50	1.00	1.02	1.00
$\nu^2 \times 10^3$, fm^{-2}	15	14	19	31
β, fm^{-1}	40	1620	1880	6400
$\lvert\phi_0\rvert^2$	0.01	0.20	0.17	0.37
$\lvert\phi_1\rvert^2$	–	1.0	1.2	3.0
$\lvert\phi_2\rvert^2$	–	–	3.0	2.0
$\lvert\phi_3\rvert^2$	–	–	–	2.5
ν_0, fm^{-1}	−0.73	−0.66	−0.64	−0.64
ν_1, fm^{-1}	–	−3.0	−3.0	−3.0
ν_2, fm^{-1}	–	–	−2.5	−2.5
ν_3, fm^{-1}	–	–	–	−3.5

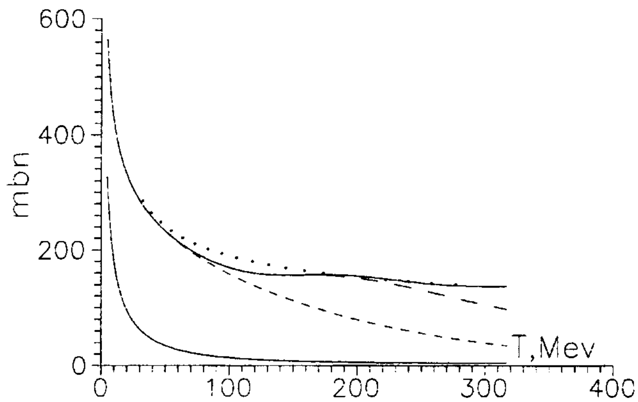

Figure 5. The total $\bar{p}p$ cross-section for the model with separated radii of annihilation and nuclear interactions. The notations are the same as for Figure 1.

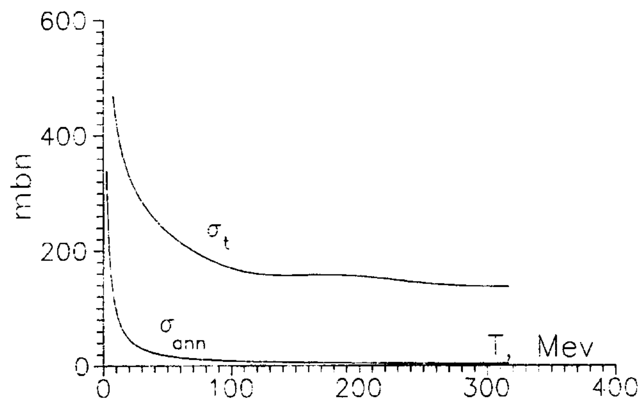

Figure 6. The total σ_t and annihilation $\sigma_{\rm ann}$ cross-sections for the $\bar{p}p$ scattering model with separated radii of annihilation and nuclear interactions.

The contribution of the annihilation cross-section to the total cross-section for the model with two radii of the interaction is shown in Figure 6.

The values of short-range interaction radii are in good agreement with theoretical predictions of other authors [7,8], namely, the annihilation radius is ~ 0.1 fm and the nuclear one is ~ 1 fm.

The infinity values of coupling constants ($\|\phi_l\|^2 = \infty$, $l = 0, 1, 2, 3$) correspond to the process of scattering by hard-core. In this case, the additional channels do not influence the scattering data. The total cross-sections of $\bar{p}n$ and $\bar{p}p$ scattering by hard core for the model with one radius of interaction are shown in Figure 7 and Figure 8, respectively. As it can be seen, the internal channel essentially influences the behavior of the cross-sections.

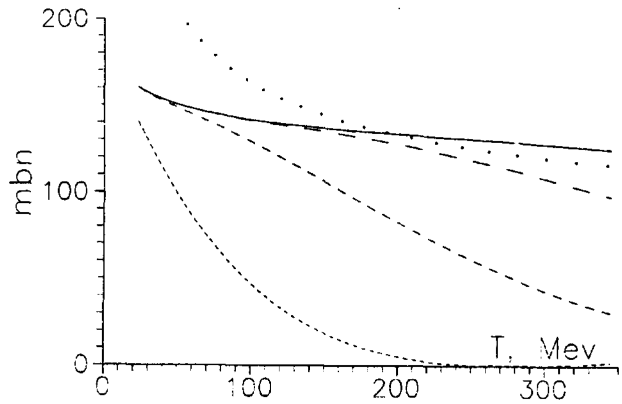

Figure 7. The total $\bar{p}n$ cross-section of scattering by hard-core for the model with one radius of interaction. The notations are the same as for Figure 1.

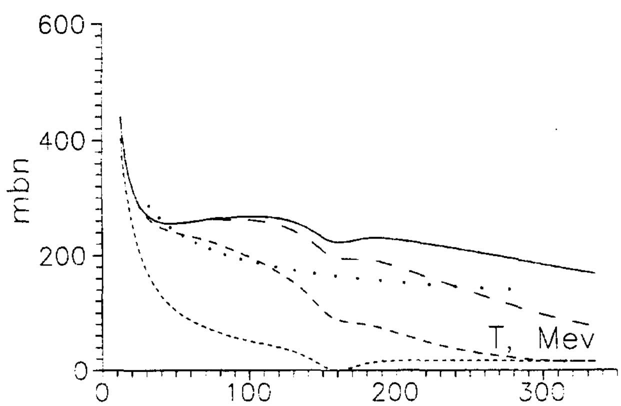

Figure 8. The total $\bar{p}p$ cross-section of scattering by hard-core for the model with one radius of interaction. The notations are the same as for Figure 1.

5. CONCLUSION

In the frame of the model, we describe the scattering length, total and elastic cross-sections both for $\bar{p}p$ and $\bar{p}n$ systems. The result of fitting shows that the higher partial waves contributions in total cross-section are essential. This fact is in good agreement with experimental results [22]. For the model with separated annihilation and nuclear interactions, the calculated interaction radii are in satisfactory agreement with other theoretical predictions [2,7,8]. As the advantage of the model, we can mention also the resonance behavior of the elastic cross-section near the threshold of annihilation which is in agreement with the predictions given in [7,8]. However, some detailed characteristics are not described satisfactorily. For example, the contribution of annihilation process to the total cross-section is less than the experimental data.

The performed parameterization of the energy-dependent pair interactions is a sound base for numerical investigation of the three-body scattering problem with annihilation channel in the frame of the Faddeev scheme combined with the extension theory approach [14]. These parameterizations may be used for a description of the bound states and the scattering processes for $\bar{p}d$, $\bar{p}t$, and $\bar{p}^3He$ systems [23] and to the annihilation processes description for $He^{++}e^-\bar{p}$ atomcule [3,4].

REFERENCES

1. C.J. Batty, *Rep. Prog. Phys.* **52**, 1165, (1989).
2. B.O. Kerbikov, L.A. Kondratyuk and M.G. Sapozhnikov, *Usp. Fiz. Nauk* **159**, 1, (1989).
3. M. Iwasaki *et al.*, *Phys. Rev. Lett.* **67**, 1246, (1991).
4. T. Yamazaki *et al.*, *Nature* **361**, 238, (1992).
5. C.B. Dover and J.M. Richard, *Phys. Rev. C* **C21**, 1466, (1980).
6. T.-A. Shibata, *Phys. Lett. B* **B189**, 232, (1987).
7. I.S. Shapiro, *Nucl. Phys. A* **A478**, 665, (1988).
8. O.D. Dalkarov, J. Carbonell and K.V. Protasov, *Yad. Fiz.* **52** (6), 1670, (1990).
9. H.R. Rubinstein and H. Stern, *Phys. Lett.* **21**, 447, (1986).
10. A.M. Green and J.A. Niskanen, *Nucl. Phys. A* **A412**, 448, (1984).
11. W. Brückner *et al.*, *Phys. Lett. B* **B169**, 302, (1986).
12. A.M. Frolov and A.J. Thakkar, *Phys. Rev. A* **A46**, 4418, (1992).
13. V.I. Korobov, Yu.A. Kuperin and S.I. Vinitsky, *Phys. Lett. B* **B315**, 215, (1993).
14. Yu.A. Kuperin and S.P. Merkuriev, Selfadjoint extensions and scattering theory for several-body systems, *Amer. Math. Soc. Transl.* **150**, 141, (1992).
15. B.S. Pavlov, *Russian Math. Survey* **42**, 127, (1987).
16. B.S. Pavlov, *Teor. Mat. Fiz.* **59** (3), 345, (1984).
17. Yu.A. Kuperin and Yu.B. Melnikov, *J. Math. Phys.* **33** (8), 2795, (1992).
18. Yu.A. Kuperin, K.A. Makarov and B.S. Pavlov, *Teor. Mat. Fiz* **69** (1), 100, (1986).
19. M.L. Goldberger and K.M. Watson, *Collision Theory*, Wiley, New York, (1964).
20. D.V. Bugg *et al.*, *Phys. Lett. B.* **B194**, 563, (1987).
21. L.A. Kondratjuk and M.G. Sapozhnokov, *Nucl. Phys. A.* **A46**, 89, (1987).
22. C. Amsler and F. Myhrer, *Annu. Rev. Nucl. Part. Sci.* **41**, 219, (1991).
23. Yu. Kuperin and E. Yarevsky, Effective annihilation potentials for the $\bar{p}d$- and $\bar{p}t$-systems, IPRT preprint, #27-94, (April 1994).